A simple model for calculating steady state tritium inventory in lithium ceramics

Alya A. Badawi
Nuclear Engineering Department, Alexandria University, Alexandria, Egypt

Lithium ceramic materials such as Li_2O, Li_2ZrO_3, $LiAlO_2$ and Li_4SiO_4 are promising fusion breeding materials in the reactor blanket. Tritium inventory in these materials needs to be accurately estimated for the design of the fusion reactor fuel cycle. A simple analytical model has been developed in this study for calculating the steady state tritium inventory inside lithium ceramic breeders by considering the processes of grain diffusion, LiOT formation and dissociation, adsorption, desorption and dissolution on the surface, and pore diffusion. The model also includes both protium and tritium species on the surface and in the pore. Comparison of the calculated tritium inventory using the model with the data obtained from three in-situ experiments: SIBELIUS, COMPLIMENT and CORELLI-2 shows that there is a reasonable agreement between the model's results and the results reported in these experiments.

تعتبر المواد الخزفية المحتوية على الليثيوم من المواد الواعدة كمولدات اندماجية في غلاف المفاعل. لابد من حساب التريتيوم الموجودة بداخل هذه المواد بدقة من أجل تصميم دورة وقود مفاعل الاندماج. فى هذه الدراسة تم تطوير نموذج تحليلي بسيط لحساب كمية التريتيوم الثابتة بداخل المولدات الخزفية لليثيوم، وذلك عن طريق اعتبار عمليات الانتشار في الحبيبات، تكوين هيدروكسيد الليثيوم، الادمصاص، المج و التفكك على السطح، والانتشار في المسام. كما اعتبر النموذج وجود فصائل بروتيوم وتريتيوم على السطح وفي المسام. تم عمل مقارنة بين كمية التريتيوم المحسوبة عن طريق النموذج والبيانات الخاصة بثلاثة تجارب مختلفة. أظهرت المقارنة اتفاق في النتائج الحسابية والمعملية.

Keywords: Lithium ceramics, Tritium inventory, Diffusion, Surface processes, LiOT

1. Introduction

The breeding blanket is a key component of the fusion reactor since it involves tritium breeding and energy extraction, both of which are critically important for the development of fusion power. Lithium-based ceramics have long been recognized as promising tritium breeding materials for fusion reactor blankets [1]. These materials have exhibited excellent tritium release, as well as thermal, physical and mechanical characteristics. In numerous in-pile experiments, lithium-containing ceramics, such as Li_2O, Li_2ZrO_3, $LiAlO_2$ and Li_4SiO_4, have performed well, showing good thermal stability and good tritium release characteristics [2]. The behavior of lithium ceramics is thus important for the performance assessment of fusion reactor blanket systems.

Estimation of the tritium inventory in the fusion reactor blanket is essential for the design of the fusion reactor fuel cycle. In order to calculate the tritium inventory in a blanket system, thorough understanding of tritium release behavior from breeding materials is required. This, in turn, requires investigation of the contribution of such tritium transfer processes as diffusion, desorption, adsorption, dissolution and isotope exchange inside different regions in the material [3].

Several time-dependent models have been proposed and used to analyze the tritium release from ceramic breeder blankets [3]. Some models, however, are of single mechanism type, that considers either diffusion (e.g. the model developed by Bertone [4] or surface reactions [5]. Other models are comprehensive fully integrated models that are too complex and time consuming for

performing analysis of the blanket and the effect of different parameters on the tritium release and inventory, MISTRAL [6,7]. The TIARA model is a simpler steady state model that takes into account many tritium processes inside the ceramic breeder [8]. However, this model is based on experimental correlation and therefore cannot be used outside the range of experimental conditions.

A simple model is required to identify the key mechanisms in tritium transport under different operating conditions, as well as examine the effect of different parameters on the tritium inventory and release. Such a model need not be time dependent, but has to include the different processes of tritium release.

A model has been developed in order to calculate the tritium inventory in a ceramic breeder blanket at steady state. The model includes the different processes present during the tritium transfer from the ceramic grains where it is generated, to the purge gas where tritium is carried away to be extracted and used as plasma fuel. Results of the developed model were compared to the experimental results in order to show its validity.

2. Model geometry and tritium processes

The model divides the solid breeder into a number of unit cells. Each cell consists of a pore that is surrounded by grains [6]. fig 1 shows a schematic diagram of the unit cell considered in the model. The number of grains per unit cell, $N_{g/p}$, can be calculated by equating the total surface area of the pores to the specific surface area (characteristic to the material under examination), which leads to [6]:

$$N_{g/p} = \frac{2\pi r_p L_p}{A_{sp}\rho v_g}. \quad (1)$$

Where; r_p is the pore radius (m), L_p is the length of the pore (m), A_{sp} is the specific surface area (m^2/kg), ρ is the material density (kg/m^3) and v_g is the volume of the grain (m^3). The number of unit cells in the ceramic, N_p, is given as [6]:

$$N_p = \frac{V\varepsilon}{\pi r_p^2 L_p}. \quad (2)$$

Where; V is the specimen volume (m^3) and ε is the porosity.

Fig. 2 shows the different processes considered in the model. The scenario of hydrogen transport in the solid breeder is: tritium is generated inside the grain and the atoms diffuse to the grain surface. While diffusing some of the tritium is trapped and forms LiOT in the grain. On the surface several reactions can take place. These include adsorption from the pore and from the grain to the surface, desorption from the surface to the pore and dissolution from the surface back to the grain. The reactions involve both tritium and protium atoms, which can combine to form H_2O, HTO, H_2, HT, T_2, or T_2O, or dissociate to stick to the surface as individual atoms.

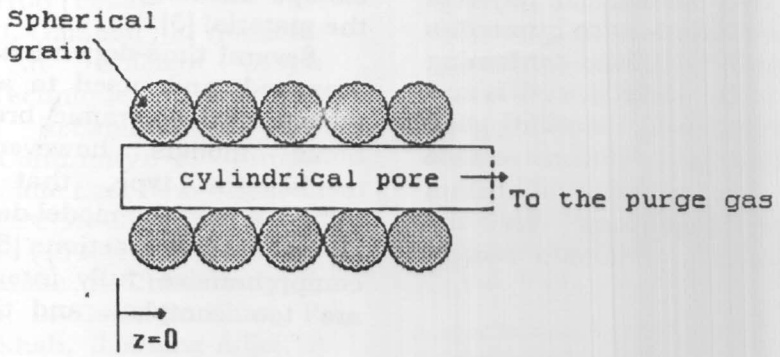

Fig. 1. Schematic diagram showing the different regions in the unit cell.

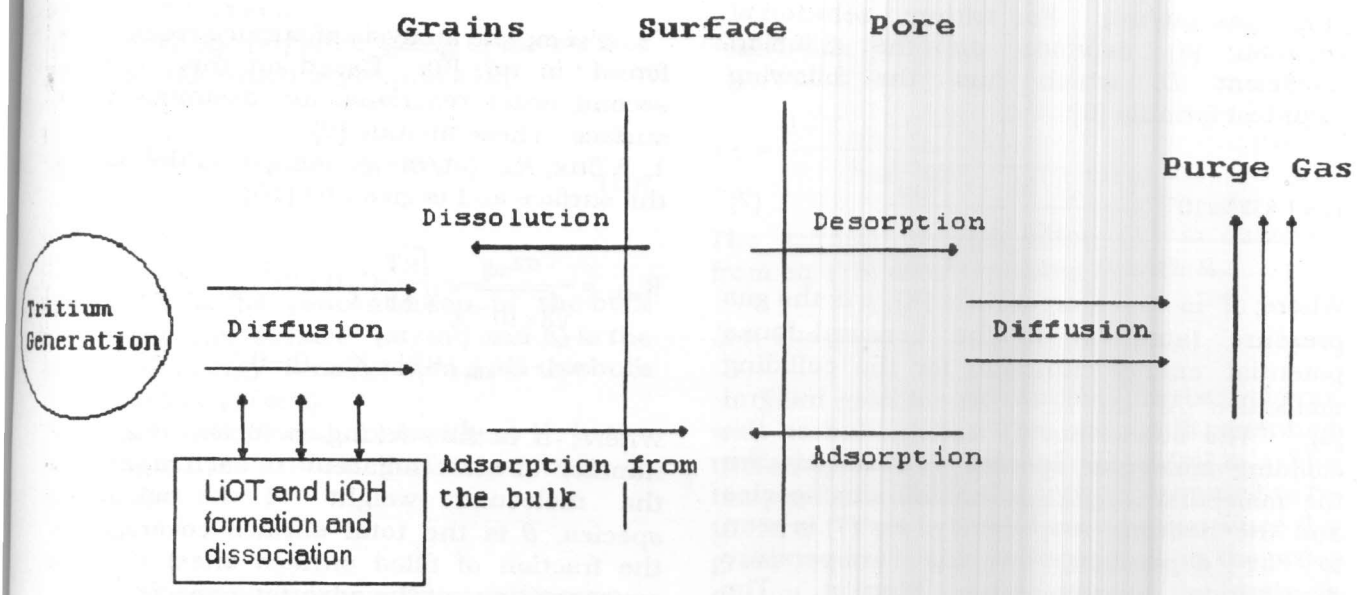

Fig. 2. Different transport processes and phenomena considered in the model.

When the atoms reach the pore, they can diffuse through the pore to the purge gas, where the helium gas carries out the tritium to be extracted and used as fuel.

A set of rate equations associated with different regimes in the unit cells is usually developed and solved simultaneously. At steady state, however, these equations are decoupled and therefore can be easily solved analytically. The tritium transfer steps considered are: (1) diffusion of tritium and formation and dissociation of LiOT inside the grain, (2) surface reactions of tritium and protium, and, (3) diffusion of tritium and protium in the pore to the purge gas. It should be noted that including protium diffusion and LiOH formation and dissociation in the grain would not produce any effect on the results due to the decoupling of the equations at steady state.

3.1 The pore

The pore is modeled as a straight cylinder of length L_p. Pore diffusion is assumed to be one-dimensional. Therefore:

$$\frac{\partial C_p}{\partial t} = \frac{\partial}{\partial z}\left(D \frac{\partial C_p}{\partial z} \right) + G_p \,. \tag{3}$$

Where; C_p is the pore concentration of either tritium or protium (at/m^3), D is the diffusion coefficient inside the pore (m^2/s) and G_p is the rate of tritium generation per unit cell (at/m^3.s). Note that for protium $G_p = 0$.

For steady state the left hand side of equation (3) equals zero. Therefore for tritium we get:

$$\frac{d}{dz}\left(D \frac{dC_{pT}}{dz} \right) = -G_p, \tag{4}$$

and for protium:

$$\frac{d}{dz}\left(D \frac{dC_{pH}}{dz} \right) = 0. \tag{5}$$

Solution of eq. (5) gives:

$$C_{pH} = C_{purge,H} \,. \tag{6}$$

$C_{purge,H}$ is the protium concentration in the purge gas (at/m^3). For tritium, solution of equation (4) depends on the diffusion coefficient D, which has the following empirical formula [6]:

$$D = 1.8583\times10^{-7}\frac{T^{3/2}\sqrt{1/M_i + 1/M_{He}}}{p\sigma_L^2\Omega_{i,j}}. \qquad (7)$$

Where; T is the temperature (K), p is the gas pressure (atm), σ_L is the Lennard-Jones potential energy function for the colliding molecules (Å) and Ω is the collision integral [6]. The subscripts (i) and (j) denote the colliding molecular species. M_i and M_{He} are the molecular weights of the diffusing species and the helium, respectively. eq. (7) is seen to be dependant on the temperature distribution inside the blanket. The temperature distribution inside the blanket is usually either uniform across the breeder, which is the case for thin breeding materials used in experiments, or has a parabolic distribution, which is the case for thick blankets. For uniform temperature distribution, solution of equation (4) gives the tritium concentration inside the pore as a function of the position z:

$$C_{pT}(z) = C_{purge,T} + \frac{G_p}{2D}\left(L_p^2 - z^2\right). \qquad (8)$$

Where $C_{purge,T}$ is the tritium concentration in the purge gas (at/m^3). For parabolic temperature distribution, eq. (4) gives:

$$C_{pT}(z) = C_{purge,T} + \frac{G_p L_p^2 p\Omega}{4.513\times10^{-3}(T_{max} - T_{min})}\left(\frac{1}{\sqrt{T_{min}}} - \frac{1}{\sqrt{T}}\right). \qquad (9)$$

Where T_{max} and T_{min} are the maximum and minimum temperatures in the pore, respectively.

3.2 The surface

A complete analysis of surface reactions is found in ref. [9]. Based on this analysis, second order reactions are assumed on the surface. These include [9]:

1. A flux, R_{ads} (at/m^2.s), going from the pore to the surface and is given by [10],

$$R_{ads} = \frac{\sigma z_{adj}}{\sqrt{8\times10^{-3}\pi}}\sqrt{\frac{RT}{M}}C_p(1-\theta)^2 \qquad (10)$$
$$\exp(-2E_{ads}/RT) = K_{ads}(1-\theta)^2$$

Where; σ is the sticking coefficient, z_{adj} is the number of sites adjacent to each atom, M is the molecular weight of the adsorbing species, θ is the total surface coverage (i.e. the fraction of filled surface sites), C_p is the concentration of the adsorbing species in the pore (at/m^3), R is the universal gas constant (J/mol.K) and E_{ads} is the activation energy of adsorption (J/mol). Note that since the pore and grain radii are very small, the temperature will be the same in the grain, on the surface, and radially in the pore. However, the temperature will vary along the length of the pore, and, therefore, the temperature of the grains and of the surface will be determined by their position along the pore.

2. A flux, R_{des} (at/m^2.s) going from the surface to the pore and is given by [11],

$$R_{des} = \frac{RN_s z_{adj} T}{A_v h}\theta^2\exp(-2E_{des}/RT) = K_{des}\theta^2. \qquad (11)$$

Where; N_s is the number of sites on the surface (at/m^2), A_v is Avogadro's number (mol^{-1}), h is Plank's constant (J.s) and E_{des} is the activation energy of desorption (J/mol).

3. A flux, R_{diss} (at/m^2.s), going from the surface back to the grain that is given by,

$$R_{diss} = \frac{RN_s z_{adj} T}{A_v h}\theta\exp(-E_{diss}/RT) = K_{diss}\theta. \qquad (12)$$

Where; E_{diss} is the activation energy of dissolution (J/mol).

4. A flux, R_β (at/m^2.s), going to the surface from the bulk which is given by [12],

$$R_\beta = \frac{3\times10^{13}}{\sqrt{N_s}} C_b(1-\theta)\exp(-E_\beta/RT) = K_\beta C_b(1-\theta). \quad (13)$$

Where; C_b is the concentration in the bulk just below the surface (at/m^3) and E_β is the activation energy for migration from the bulk to the surface (J/mol).

For steady state conditions with no H_2 in the purge gas, the tritium surface coverage is equal to [9]:

$$\theta_T = \frac{-K_{ads,T} + \sqrt{K_{ads,T}^2 + (G + K_{ads,T})(K_{des} - K_{ads,T})}}{K_{des} - K_{ads,T}}, \quad (14)$$

where $K_{ads,T}$ is obtained from eq. (10) with $C_p = C_{pT}$ and $M = M_T$, and G is the rate of tritium generation per unit surface area (at/m^2.s).

The tritium bulk concentration at the surface, $C_{b,T}$ can be obtained from [10]:

$$C_{b,T} = \frac{G + K_{diss}\theta_T}{K_\beta(1-\theta_T)}. \quad (15)$$

When H_2 is added to the purge gas, the surface coverage is divided to θ_T of the tritium and θ_H of the protium. The total surface coverage, θ_{tot}, is equal to:

$$\theta_{tot} = \theta_T + \theta_H. \quad (16)$$

The total and tritium surface coverage can be obtained as a function of different coefficient [10]:

$$\theta_{tot} = \frac{K_{tot} - \sqrt{K_{tot}^2 - (G + K_{tot})(K_{tot} - K_{des})}}{K_{tot} - K_{des}}, \quad (17)$$

where;

$$K_{tot} = K_{ads,T} + K_{ads,H} \quad \text{and} \quad (18)$$

$$\theta_T = \frac{G + K_{ads,T}(1-\theta_{tot})^2}{K_{des}\theta_{tot}}. \quad (19)$$

The tritium concentration $C_{b,T}$ is obtained from eq. (15) after replacing θ_T with θ_{tot}.

3.3. The grain

The grains are assumed to be spheres with radius r_g(m). The tritium is generated uniformly at a rate of G_g (at/m^3.s). The temperature inside the grain is assumed to be uniform. This is a valid assumption since the grain radius is always very small, in the order of μm. The temperature of the grain is determined by its position along the pore. For one-dimensional diffusion:

$$\frac{\partial C_d}{\partial t} = \frac{1}{r^2}\frac{\partial}{\partial r}\left(r^2 D_g \frac{\partial C_d}{\partial r}\right) + G_g - \frac{\partial C_s}{\partial t}, \quad (20)$$

and

$$\frac{\partial C_s}{\partial t} = k_{for} C_d - k_{dsn} C_s. \quad (21)$$

Where; C_d is the concentration of the diffusing tritium (at/m^3), C_s is the LiOT concentration (at/m^3), D_g is the grain diffusion coefficient (m^2/s), k_{for} is the rate of LiOT formation (at/s) and k_{dsn} is the rate of LiOT dissociation (at/s). At steady state equations (20) and (21) are decoupled and can be solved independently to give:

$$C_d = C_{b,T} + \frac{G_g}{6D_g}\left(r_g^2 - r^2\right), \quad (22)$$

and

$$C_s = \frac{k_{for}}{k_{des}} C_T. \quad (23)$$

4. Calculation steps

The pore is divided into a number of nodes N_z. For each node the following is calculated:

1. The temperature (uniform or parabolic).
2. The tritium and protium concentrations in the pore at the node from eqs. (6) and (8) or (9), depending on the temperature distribution.
3. The tritium surface coverage from equation (14) (if there is no H_2 in the purge gas) or (19) (if H_2 is present).
4. The tritium concentration at the surface of the grain from eq. (17).
5. The diffusing tritium and LiOT concentrations inside the grains from eqs. (22) and (23).

In each region the inventory will be equal to the integration of the tritium concentration over the volume of the region. Therefore:

$$I_{pore} = \pi r_p^2 C_{pT} \frac{L_p}{N_z}, \tag{24}$$

$$I_{grain} = v_g \left[C_{bT} + \frac{G_g r_g^2}{15 D_g} \right] \frac{N_{g/p}}{N_z}, \tag{25}$$

$$I_{LiOT} = \frac{k_{for}}{k_{dsn}} I_{grain} \quad \text{and} \tag{26}$$

$$I_{surface} = \theta_T N_s \frac{A_{sp} \rho V}{N_z}. \tag{27}$$

The tritium inventory in the unit cell is equal to the sum of the inventories in different regions, i.e.,

$$I_{tot} = \sum_{N_z} \left(I_{pore} + I_{grain} + I_{LiOT} + I_{surface} \right). \tag{28}$$

The tritium inventory in this case is given as the total number of tritium atoms. In terms of tritium activity, the inventory (Bq) will be equal to:

$$I_{tot,Bq} = I_{tot} \lambda. \tag{29}$$

λ is the tritium time constant, which is equal to 1.78×10^{-9} sec^{-1}.

5. Comparison between model results and experimental data

In order to show the validity of the developed model, it is necessary to compare its results with different experimental data. Three different in-situ tritium release experiments were investigated. These are SIBELIUS [13,14], COMPLIMENT [15] and CORELLI-2 [16]. Table 1 shows the different experiments considered. The ceramic breeders used were Li_2O and $LiAlO_2$. The purge gas in all three experiments consisted of helium + 0.1% protium.

A comparison between the model and experimental data is shown in table 2. Although the tritium generation and temperature in SIBELIUS were specified, the reported tritium inventory differed when the different irradiation were performed on the same samples under the same conditions. The experiment gave a number of results ranging from 41.3 - 43.3 MBq for the Li_2O sample. The model predicted ~47 MBq, which is in agreement with the experiment. In the case of $LiAlO_2$ samples, the experiment reported an inventory between 136-236 MBq. The model predicted an inventory of 250 MBq, which is 5-45% higher than the experiment. The large differences in the experimental data in this case makes the comparison meaningless. A probable explanation for this is that steady state was not reached in some of the cases reported.

In the COMPLIMENT experiment, $LiAlO_2$ samples with different grain sizes and porosities were irradiated. When the 0.6 μm samples, were irradiated at 600°C, the measured inventory was 3076 MBq. The calculated inventory was 4491, which is 31%

Table 1
Experimental data of different in-situ tritium release experiments

Experiment	Material	Geometry	Porosity (%)	Grain Size (μm)	Purge Gas
SIBELIUS [13,14]	Li_2O	Pellets	20	20	He + 0.1% H_2
	$LiAlO_2$		25	0.4	
COMPLIMENT [15]	$LiAlO_2$	Pellets	21.5, 20	0.51, 0.48	He + 0.1% H_2
CORELLI-2 [16]	$LiAlO_2$	Pellets	20	0.6, 12	He + 0.1% H_2

Table 2
Comparison between model and experimental results

Experiment	Temperature (°C)	Tritium Generation MBq/day	Calculated Inventory MBq	Experimental Inventory MBq
SIBELIUS Li_2O [13,14]	500	4220	46.95	41.33-43.31
SIBELIUS $LiAlO_2$ [13,14]	550	4000	249.2	136-236
COMPLIMENT $LiAlO_2$ [15]	450	3076	3752.7	3076
COMPLIMENT $LiAlO_2$ [15]	600	3076	4491	3076
CORELLI-2 $LiAlO_2$ [16]	600	3637	95.47	91
CORELLI-2 $LiAlO_2$ [16]	500	3059	1781.9	943-1937

higher than the data. The 12 μm samples irradiated at 450°C had an inventory of 3076 MBq. The calculated inventory was 3752.7 MBq, a value 18% higher than the experiment. Note that in this experiment, the dimensions of the specimens were not accurately specified.

In the CORELLI-2 experiment, $LiAlO_2$ pellets were irradiated at 500°C and 600°C. Irradiation of 0.6 μm-grain pellets produced an inventory of 91 MBq. The calculated inventory was 95.5 MBq, which is 5% higher than the experimental value. For the cases of 12 μm grains irradiated at 500°C the calculated inventory was 1782 MBq. The measured inventory ranged between 943-1937 MBq, which produces a difference between –47% and 8% from the calculations. The above comparison between the calculations and experimental data shows that in most cases the calculated results are higher than the experimental values. This can be explained by noting that the irradiation time in the experiments is small for modeling to be accurate in its early stage. This means that the samples do not actually reach the steady state that is depicted in the present model. The fact that the samples do not reach steady state can be clearly seen from the CORELLI-2 and the SIBELIUS experiments. When similar samples were irradiated under the same conditions, the measured tritium inventories inside these samples were not the same.

6. Summary

A model has been developed to calculate the tritium inventory in a blanket under steady state conditions by considering the processes of grain diffusion, LiOT precipitation, surface adsorption, desorption and dissolution, and pore diffusion. Both tritium and protium species were considered in the model.

The model was used to estimate the tritium inventory in Li_2O and $LiAlO_2$ samples. Different inputs to the model were obtained

from three in-situ experiments: SIBELIUS, COMPLIMENT, and CORELLI-2.
Calculations using the model of this study give a reasonable agreement with the tritium inventory measured in those experiments.

References

[1] C.E. Johnson, K. Noda and N. Roux, "Ceramic Breeder Materials: Status and Needs," J. Nucl. Mater., 140-148, 258-263(1998).

[2] R.F. Mattas and M.C. Billone, "Materials for Breeding Blankets," J. Nucl. Mater., 72-81, 233-237(1996).

[3] G. Federici, A.R. Raffray, M.C. Billone, C.H. Wu, S. Cho and M.A. Abdou, "An Assessment of Models for Tritium Release from Ceramic Breeders for Blanket Analysis Applications," J. Nucl. Mater., 1003-1009, 212-215(1994).

[4] P.C. Bertone, "The Kinetics that Govern the Release from Neutron-Irradiated Lithium Oxide," J. Nucl. Mater., 281-292, 151(1988).

[5] D. Yamaki, S. Tanaka and M. Yamawaki, "Modeling of the Surface Reaction of Tritium Release from Lithium Ceramics," J. Nucl. Mater., 917-922, 212-215(1994).

[6] G. Federici, A.R. Raffray and M.A. Abdou, "MISTRAL: A Comprehensive Model for Tritium Transport ' in Lithium-Base Ceramics- Part I: Theory and Description of Model Capabilities," J. Nucl. Mater., 185-213, 173(1990).

[7] A. Badawi, "Modeling and Analysis of Time-Dependent Tritium Transport in Lithium-Containing Ceramics," Ph.D. Thesis, UCLA, 1993.

[8] M.C. Billone, "Thermal and Tritium Transport in Li_2O and $LiZrO_3$," J. Nucl. Mater., 1462-1466, 233-237 (1996).

[9] A. Badawi, "Analysis of First and Second Order Surface Reactions in Ceramic Breeders," AEJ, 39, pp. 255-263 (2000).

[10] A. Badawi, A.R. Raffray and M.A. Abdou, "Analysis of Tritium Transport Mechanisms at the Surface of Lithium Ceramics," Fusion Technol., 1939-1943, 21 (1992).

[11] M. Boudart and G. Djéga-Mariadassou, "Kinetics of Heterogeneous Catalytic Reactions," Princeton University Press, Princeton (1984).

[12] M.A. Pick and K. Sonnenberg, "A Model for Atomic Hydrogen-Metal Interactions-Application to Recycling, Recombination and Permeation," J. Nucl. Mater., 208-220, 131 (1985).

[13] J.P. Kopasz, C.E. Johnson and D.L. Baldwin, "Performance of Ceramic Breeder Materials in the SIBELIUS Experiment," J. Nucl. Mater., 259-264, 219 (1995).

[14] C.E. Johnson, D.L. Baldwin and J.P. Kopasz, " Tritium Release from Beryllium Discs and Lithium Ceramics Irradiated in the SIBELIUS Experiment," J. Nucl. Mater., 966-970, 212-215 (1994).

[15] C. Alvani, P.L. Carconi, S. Casadio and A, Moauro, "Tritium Removal from Various Lithium Aluminates Irradiated by Fast and Thermal Neutrons (COMPLIMENT Experiment)," J. Nucl. Mater., 259-265, 208 (1995).

[16] F. Alessandrini, C. Alvani, S. Casadio, M.R. Mancini and .A. Nannetti, "In-Situ Tritium Release (CORELLI-2 Experiment) and Ex-Reactor Ionic Conductivity of Substoichiometric $LiAlO_2$ Breeder Ceramics," J. Nucl. Mater., 236-244, 224 (1995).

Received October 11, 2000
Accepted January 1, 2001